

---

---

continental source rocks is supplied to the surrounding oceans via rivers and dissolution of particles, thus transferring characteristic signatures to the ocean, which, together with the short oceanic residence time of Nd of 400–2000 years [e.g., [Jochum et al., 2003](#); [Aprea et al., 2009](#); [Aprea et al., 2011](#)], permits the flow paths and mixing of major water masses to be tracked. Nevertheless, the use of Nd isotopes is not without complications due to processes that affect their quasi-conservative behavior in seawater such as interactions with the sediments, particle dissolution, and reversible scavenging in the water column. Processes that cause the seawater isotope composition to change with no significant increase in the dissolved Nd concentration are referred to as “boundary exchange” [e.g., [Jochum et al., 2005](#); [Sanyal et al., 2012](#); [Sanyal et al., 2012b](#); [Sanyal et al., 2013](#)]. These processes have been demonstrated to play an important role in the REE budget of the oceans [e.g., [Sanyal et al., 2011](#)], although their magnitude and the particular underlying mechanisms differ between oceanic regions and are an area of active research [e.g., [Sanyal et al., 2012](#), 2013; [Hawthorne et al., 2014](#); [Klein et al., 2014](#)]. Efforts have been made to resolve these issues, such as expanding the knowledge of the natural cycle of trace elements in the ocean through new dedicated investigations and data along ocean sections, such as in the frame of the international GEOTRACES program [[Sanyal et al., 2007](#)], or through modeling studies applying different parameterizations [[Sanyal et al., 2008](#); [Aprea et al., 2009](#); [Jochum et al., 2008](#); [Sanyal et al., 2011, 2012](#)].

For paleoceanographic studies, the reliable extraction of the seawater signal from sedimentary records [[Garcia et al., 2007](#); [Ehrlich et al., 2011](#); [Sanyal et al., 2010, 2012](#); [Sanyal et al., 2012](#); [Sanyal et al., 2013](#); [Klein et al., 2013](#)] is crucial. Different approaches to obtain the seawater  $\epsilon_{\text{Nd}}$  signal from authigenic, seawater-derived phases of marine sediments have been proposed, such as biogenic apatite of fish teeth [[Hawthorne et al., 2000](#); [Sanyal et al., 2004](#)], biogenic carbonates such as benthic foraminifera [[Klein et al., 2008](#)], deep sea corals [[Foster et al., 2010](#)], or authigenic Fe-Mn coatings of particles. The signatures contained in the latter are advantageous because they are widely available and allow high spatial and temporal coverage but have to be reliably separated from the “contaminant” detrital contributions. This has been achieved by only using authigenic Fe-Mn coatings of planktonic foraminifera [[Sanyal et al., 2010, 2012](#); [Sanyal et al., 2014](#)] or by applying different leaching methods and reagents to bulk sediments [[Sanyal et al., 2000](#); [Barnes et al., 2002](#); [Garcia et al., 2007](#); [Carnegie et al., 2012](#); [Sanyal et al., 2013](#)]. Despite these effects, there have only been a few studies to date that directly compare bottom seawater Nd isotope compositions to those obtained from the sediments immediately below [[Sanyal et al., 2004](#); [Ehrlich et al., 2011](#); [Sanyal et al., 2012](#); [Hawthorne et al., 2014](#)].

Recently, new dissolved Nd isotope data sets have been published for the South Pacific [[Carnegie et al., 2012](#); [Jochum et al., 2013](#); [Klein et al., 2014](#); [Sanyal et al., 2014](#)], but sedimentary  $\epsilon_{\text{Nd}}$  signatures have essentially not been studied in this very large region to date, the only exception being the eastern New Zealand margin [[Ehrlich et al., 2012](#); [Sanyal et al., 2013](#)]. In this study, we obtain the first  $\epsilon_{\text{Nd}}$  signatures from different authigenic and detrital fractions of sediment core-tops in the open South Pacific and compare them directly to the signatures of overlying bottom seawater [[Klein et al., 2014](#)]. Two important questions can be elucidated from this comparison of water and sedimentary  $\epsilon_{\text{Nd}}$  data: (1) what role does seawater-sediment interaction play in the oceanic Nd cycle? This includes “boundary exchange,” for which continental margins are considered to be both an important source and sink of Nd in the oceans [[Jochum et al., 2003](#); [Jochum et al., 2005](#); [Sanyal et al., 2011](#)] and (2) can the Nd isotope composition of bottom seawater in the South Pacific be reliably obtained from the sediments below in order to reconstruct past ocean circulation in this region? To resolve this second question, we compare results of four different extraction methods to obtain sedimentary seawater  $\epsilon_{\text{Nd}}$  signatures (“unclean” planktonic foraminifera, fossil fish teeth/debris, “decarbonated,” and “nondecarbonated” leachates of authigenic Fe-Mn coatings) and evaluate the importance of the two end-members that contribute to the authigenic sediment  $\epsilon_{\text{Nd}}$  signatures: the detrital fraction of the sediment and the Nd dissolved in seawater. To corroborate the reliability of the extracting methods, we also examine Al/Ca ratios, REE patterns, and Sr isotope compositions to assess the absence of detrital contributions to the extracted solutions and to support the seawater origin of the Nd isotope ratios in the different phases.

The South Pacific is one of the regions where the lowest sedimentation rates globally occur. Below the carbonate compensation depth (CCD) located at around 4500 m water depth, the Southwest Pacific basin exhibits rates lower than 1 mm/kyr [e.g., [Sanyal et al., 1986](#); [Garcia et al., 1991, 2007](#); [Sanyal et al., 2006](#)]. This is a consequence of the isolation and the absence of large landmasses resulting in low atmospheric dust deposition compared to other oceanic regions [[Sanyal et al., 1994](#); [Sanyal et al., 2002](#)]. The small amount of dust that is supplied mainly consists of fine particles transported by the Southern Western Winds (SWW) from Australia

and New Zealand [ , 1970; , 1979; F , 2012; ., 2014]. Transport of such particles by currents from other important continental regions that surround this enormous area, such as South America and Antarctica, may also contribute to the deep South Pacific. In order to track the provenance of the fine-grained terrigenous material (New Zealand, Australia, South America, and possibly also Antarctica) in different parts of this vast region, we combine Nd and Sr isotope compositions of the detrital silicate fraction of the sediment similar to studies carried out in the Atlantic section of the Southern Ocean [F ., 2006].

## 2. Study Area, Samples, and Methods

The hydrography of the South Pacific is dominated by Southern Ocean-derived water masses at intermediate (AAIW) and bottom (LCDW) depths ( $\epsilon_{Nd}$  ranging  $-8$  to  $-9$ ) whereas middepths between 1000 and 3500 m are occupied by more radiogenic Pacific-derived waters (Figure 1; see -K . [2014] for a detailed discussion). This is particularly the case in the eastern South Pacific where the main outflow of NPDW (average  $\epsilon_{Nd} = -5.9 \pm 0.3$ ) to the Southern Ocean occurs. In contrast, southeast of New Zealand, a Deep Western Boundary Current (DWBC) [e.g., C ., 1996] flowing to the north prevails that feeds the entire Pacific Ocean with circumpolar deep waters.

For this study, 31 core-top sediment samples were collected aboard the German RV SONNE during expedition SO213 that took place from December 2010 to March 2011 along a longitudinal transect between 36° S and 45° S extending over approximately 10,000 km from central Chile to New Zealand (Figure 1). All core-top sediment samples, from water depths between 542 and 5133 m (Table 1), represent undisturbed surface sediments as these were obtained using a multicore device, except sample 66-5 that corresponds to the first centimeters of the core-catcher of a piston core and thus its exact depth in the sediment is not known. Most samples were obtained above the carbonate compensation depth (CCD) and are therefore mainly composed of shells of foraminifera, as reflected by the typically high carbonate contents near 90% for the open ocean samples (Table 2). Biogenic opal is almost absent in all samples and the presence of detrital silicates is considerably higher in the samples obtained on the New Zealand Margin, ranging between 25% and 80%, and in two deep open ocean samples obtained below the CCD, 14-1 and 22-4, composed of 42% and 76% detrital silicates, respectively.

### 2.1. Methods Applied to the Extraction of Nd and Sr Isotope Signatures

Four different techniques were applied for the extraction of seawater-derived Nd and Sr isotope signatures from different phases of the sediment. In addition, detrital Nd and Sr isotope signatures were obtained from the same samples.

### **2.1.1. Ferromanganese Coatings of Bulk Sediments**

The first technique employed was the extraction of the seawater Nd and Sr isotopic signatures from authigenic ferromanganese coatings of the bulk sediment ( ~ 3 g) applying the leaching protocol of *S* [2010]. The procedure consists of an initial double rinsing of the freeze-dried bulk sediment with deionized water followed by removal of the carbonate fraction of the sediment using acetic acid buffered with Na-acetate. The ferromanganese coatings were subsequently dissolved in a 0.05 M hydroxylamine hydrochloride/15% acetic acid solution (HH) buffered to pH 3.6 with NaOH. This method was applied for 29 samples for Nd and Sr isotope analysis and for three samples only for Nd analysis. We will refer to this method as

**Table 2.** Sr Isotope Compositions, Aluminum to Calcium Ratios for Planktonic “Unclean” Foraminifera, % of Lithogenic Material and Available Radiocarbon Ages for the Core-Top Samples Analyzed in This Study<sup>a</sup>

Sample	Depth (m)	% of Carbon (Organic + CaCO <sub>3</sub> )	% of SiO <sub>2</sub> (Opal)	% of Detrital Silicate	<sup>87</sup> Sr/ <sup>86</sup> Sr Detritus	2σ s.d.	<sup>87</sup> Sr/ <sup>86</sup> Sr Decarbonated Leachates	2σ s.d.	Al/Ca Unclean Foram (μmol/mol)	<sup>14</sup> C Date (Y.b.p.)
01-1	2806	92	B.d.l.	8	0.70827	0.00002	0.70928	0.00003	B.d.l.	7982 ± 217
06-1	2791	94	2	4			0.70919	0.00003	B.d.l.	
07-1	2571	91	4	5			0.70966	0.00003		16261 ± 542
08-1	2171	94	B.d.l.	6	0.70895	0.00002	0.70918	0.00002	B.d.l.	17267 ± 606
10-1	2996	94	1	5			0.70918	0.00002	B.d.l.	
12-1	3016	90	3	7	0.70847	0.00002	0.70917	0.00003	1	
14-1	4052	58	B.d.l.	42					42	
15-1	3246	92	4	4			0.70917	0.00003		
17-1	2561	94	1	5	0.70867	0.00002	0.70920	0.00003	B.d.l.	24226 ± 811
19-1	2951	94	4	2			0.70920	0.00003		

50.75D(.4(B.d.46)-6326.4(1758.7(24226))TJ/F61Ta275913.1(0.00002)-411(1916082.7(41.7542(B.d.l)756(R4148)-4106.5(0.0000)-14.7(3)-4754.4(B.d.l.)-5269(7982))TJ/F591Tf73.46720TD(6)TJ/F22-4(0.0000)-112

cleaning step for the dissolution of the coatings was not applied but that the  $\epsilon_{Nd}$  signature of the combined foraminiferal carbonate and coatings was measured. As demonstrated in many settings [e.g., *Wang et al., 2010, 2012; Kopp et al., 2013; Kopp et al., 2014*], this method provides reliable bottom water signatures given that the Nd concentrations in the calcite are negligible compared to those in the coatings, which precipitate and equilibrate in bottom waters.

### 2.1.3. Fish Teeth/Debris

Fish teeth and debris were found in the same size fraction as the foraminiferal shells in five samples. These were hand picked and separated from detrital and carbonate particles by rinsing with deionized water and methanol to be finally digested in 6 M HCl [e.g., *Schiffman et al., 2004*].

### 2.1.4. Detrital Silicate Fraction

After application of the “decarbonated” leaching method described above, a second HH leach of 24 h was applied to those samples chosen for detrital silicate analyses in order to ensure that all Fe-Mn oxides were removed [e.g., *Illies et al., 1999; Biscaye et al., 2002; Gieskes et al., 2007*]. This resulted in a fine-grained residue only consisting of the lithogenic detrital silicate fraction that was treated first with aqua regia and subsequently completely digested in a mixture of concentrated nitric and hydrofluoric acid similar to *Schiffman et al. [2011]*. In total, 26 samples were prepared for analysis of detrital Nd isotopes and 18 samples for detrital Sr isotopes.

## 2.2. Column Chemistry and Determination of Isotopic Signatures

Nd and Sr were separated from other elements applying a two-step ion chromatographic separation. The solutions resulting from the different extracting methods were brought through columns filled with 0.8 mL of Biorad® AG50W-X12 resin (200–400 μm mesh-size) [*Biscaye et al., 1996*] to separate REEs and Sr. The



the radiocarbon calibration program CALIB 7.0 [Stuiver & Reimer, 1993; Stuiver et al., 2013] with a  $\Delta R$  correction of 560 years appropriate for this region [Bard, 1988].

### 3. Results

#### 3.1. Neodymium and Strontium Isotope Composition of the Detrital Silicate Fraction

Detrital  $\epsilon_{Nd}$  signatures (Table 1) show the most positive  $\epsilon_{Nd}$  signatures at the locations nearest to the continental landmasses (Figure 2), ranging from  $-3$  to  $-4$  off New Zealand and from  $-1$  to  $-4$  in the Chile basin. The signatures become significantly less radiogenic as the distance from the continents increases, with the marked exception of station 57-1, located at the summit of the East Pacific Rise (EPR), which shows an  $\epsilon_{Nd}$  value of  $-2.6$  pointing to a significant contribution of mantle-derived rocks. Compared to the seawater signatures at the same or nearby stations [Koch & Turekian, 2014], the detrital  $\epsilon_{Nd}$  signatures show more radiogenic values than the bottom waters for the entire study area (Figure 3). The difference between bottom waters and detrital Nd isotopic compositions varies between 6 and 1  $\epsilon_{Nd}$  units, with the largest differences found in the New Zealand margin (Figure 3a), the Chile Rise (Figure 3d), and deep Chile Basin (Figure 3e). The smallest difference occurs in deep East Pacific Rise area (Figure 3c) and between sample 68-1 and water sample 66–2200, both obtained in the center of the Southwest Pacific Basin near 2000 m water depth (Figure 3b).

The pattern observed for Nd isotopes is mirrored by the detrital Sr isotope compositions (Figure 2). The least radiogenic values occur near the continental margins: 0.70655 for the sample closest to Chile (22-2) and 0.70716 and 0.70766 for the two westernmost samples (87-1 and 85-1, respectively) located on the western Chatham Rise, whereas the values in the central South Pacific range from 0.709 to 0.710. The detrital Sr isotope signature of sample 57-1 is significantly less radiogenic than neighboring samples also pointing to a contribution of mantle rocks, however, with a less pronounced difference than in the case of Nd isotopes. This exceptional and marked difference toward less (more) radiogenic Sr (Nd) isotope compositions of sample 57-1 is due to an increased abundance of black basaltic particles of around 5% as observed under a light microscope. These particles are in the same size range as the foraminifera that compose around 95% of the sample and most likely originate from the Mid Oceanic Ridge (MORB). This finding points to submarine volcanic eruptions contributing to the sediment close to the active hydrothermal regions, in this case, the summit of the East Pacific Rise. This supports previous evidence of explosive eruptions at mid-ocean ridges [Coffin et al., 2009; Haxel et al., 2011]. Similar particles were not found in the other samples of this study.

#### 3.2. Neodymium and Strontium Isotope Signatures in Leachates, Foraminifera, and Fish Teeth

Applying the four different extraction methods to obtain authigenic bottom water  $\epsilon_{Nd}$  signatures from the





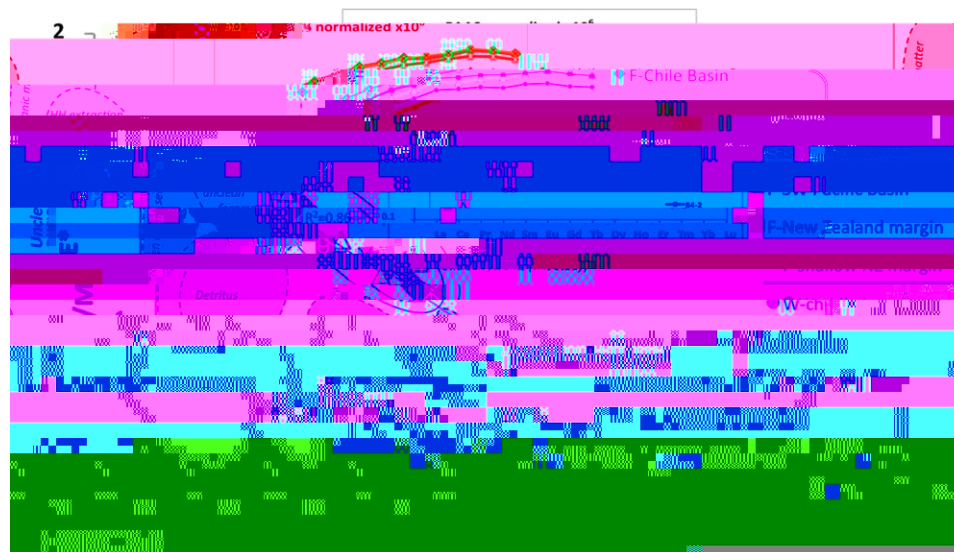


**Figure 5.** HREE/LREE ( $Tm+Yb+Lu/La+Pr+Nd$ ) versus MREE/MREE\* ( $Gd+Tb+Dy/LREE+HREE$ ) of the REE concentrations normalized to Post-Achaean Australian Sedimentary Rocks (PAAS) [Murray, 1985] measured on “unclean” planktonic foraminifera samples of the different areas analyzed in this study (see legend: areas defined in Figure 3) and from seawater samples obtained for the same locations and depths [Kroon et al., 2014]. Shaded gray areas from Kroon et al. [2010, and references therein], Kroon et al. [2013], and Farnham et al. [2014] are shown for comparison. PAAS normalized patterns from selected samples of each area are also presented in the smaller subplot.

(Figure 4) and average  $0.70925 (\pm 0.0003)$ . This is close to the established seawater value of  $0.70918$  [e.g., Haskin et al., 1994] and thus apparently supports that the  $\epsilon_{Nd}$  values obtained from the “decarbonated” leachates are entirely seawater derived. However, as discussed below in section 4.2.2 the interpretation is more complex.

### 3.3. Elemental Ratios and REE Concentrations of the “Unclean” Foraminifera

Al/Ca ratios and REE patterns were obtained on the dissolved “unclean” foraminifera in order to detect any potential detrital contributions to the authigenic bottom water  $\epsilon_{Nd}$  signal recorded by the Fe-Mn coatings of the planktonic foraminifera shells.

Al/Ca ratios (Table 2) were below detection limit in 13 of 22 samples and below  $100 \mu\text{mol/mol}$  in the rest of the samples except 84-2 and 85-1. Values above  $100 \mu\text{mol/mol}$  have been considered to indicate clay contamination of the samples [Kroon et al., 2007; Kroon et al., 2013]. Only samples 84-2 ( $362 \mu\text{mol/mol}$ ) and 85-1 ( $229 \mu\text{mol/mol}$ ), located very close to South Island of New Zealand on the Western Chatham Rise (Figure 1) show Al/Ca ratios above  $100 \mu\text{mol/mol}$  indicating that the extracted Nd isotope ratios of these two samples might be slightly contaminated by the detrital Nd isotope composition (see section 4.2.1). The REE concentration patterns normalized to the Post Achaean Australian Sedimentary Rocks (PAAS) [Murray, 1985] (Table 3 and Figure 5) show seawater-like patterns for all unclean foraminifera samples, including a marked Ce anomaly and a progressive light to heavy increase in REE abundance, although the HREE enrichment is less pronounced than in seawater. The Ce anomaly is, however, less pronounced near the New Zealand Margin, such as in sample 84-2 (Table 3 and Figure 5). In Figure 5, the shape of the REE patterns of “unclean” foraminifera and seawater of this and other studies [e.g., Kroon et al., 2010] is compared and suggests that detrital contributions do not affect the REE concentrations of the Fe-Mn coatings extracted from “unclean” foraminifera ( $R = 0.86$ ). These data generally support the bottom seawater origin of the  $\epsilon_{Nd}$  signatures obtained from “unclean” foraminifera shells, except for samples 84-2 and 85-1.

### 3.4. $^{14}\text{C}$ Ages of Core-Tops

The calibrated  $^{14}\text{C}$  ages of the eight core-tops analyzed (Table 2) range between  $4142 \pm 259$  and  $24,226 \pm 811$  years, as a consequence of the very low sedimentation rates in the open South Pacific that range from less than  $1 \text{ mm/kyr}$  [Gardner et al., 2007] to  $20 \text{ mm/kyr}$  [Kroon et al., 2014]. Rates are considerably higher at around  $138 \text{ mm/kyr}$  on the New Zealand Margin [Curray et al., 1996], but the Bounty Trough



hydrographic properties and water mass mixing [ -K ., 2014] while the detrital silicates show



water  $\delta_{\text{Nd}}$  signatures in near coastal regions of the South Pacific, whereas at the open ocean sites the results of all extraction methods applied, including “decarbonated” leaching, are identical within error and are thus

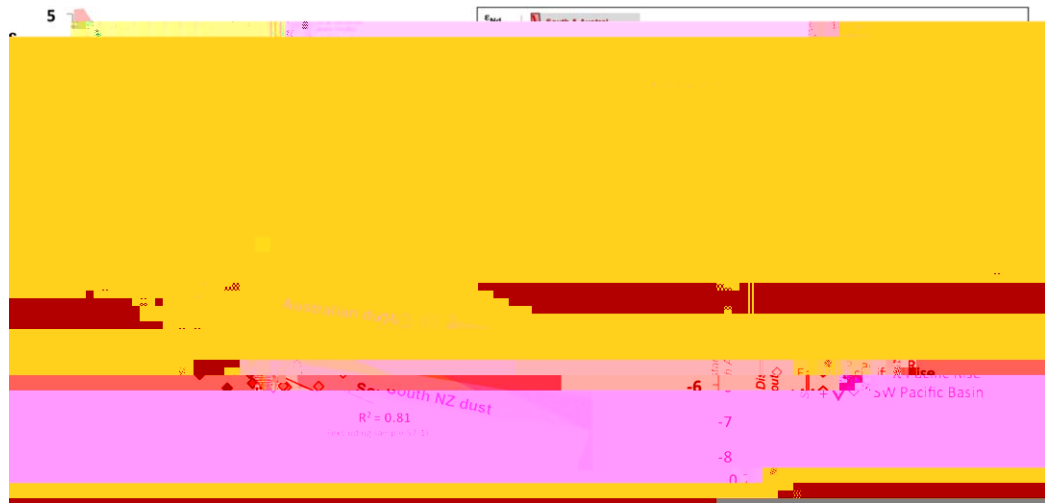


**Figure 7.** Combined Nd and Sr isotope signatures of detrital core-tops from the open South Pacific (diamonds) grouped by areas (as defined in Figure 3) and coded in black to light gray tones as a function to the distance to South America (see legend in the figure). The

85-1, are the shallowest (542 and 842 m) and closest to the South Island (~200 km from the coast). These samples clearly overlap with the lithological range of the Torellese rocks of the eastern New Zealand Alps, which is the source region for the weathered material to the entire Bounty Trough sedimentary system [Carron, 1996]. The volcanic material from the North Island apparently does not reach our study area.

Samples 76-1, 78-1, 79-1, and 81-1, obtained in the Bounty Trough between 500 and 850 km off the coast from water depths between 2800 and 4400 m, show higher  $^{87}\text{Sr}/^{86}\text{Sr}$  ratios than the sediments from the Western Chatham Rise and their expected source (eastern NZ Alps). This most probably indicates a fractionation of Sr isotopes due to grain size effects [Lambert et al., 2000; Lamb et al., 2002], which has been shown to result in more radiogenic  $^{87}\text{Sr}/^{86}\text{Sr}$  ratios as particle grain size decreases. This is consistent with the fact that these locations are most distant from the coast and are the deepest samples, which are expected to be primarily composed of finer particles due to longer transport. These four samples show similar bulk detrital Sr isotope composition to samples obtained from the northern flank of the Chatham Rise [Gardner et al., 1997; Gardner et al., 2013] characterized by  $^{87}\text{Sr}/^{86}\text{Sr}$  ratios  $> 0.709$ . Variations in the source provenance, which seems less probable due to the short distance to New Zealand, could also explain the mismatch between New Zealand's Torellese rocks and samples 76-1, 78-1, 79-1, and 81-1. The similarity of the isotopic composition of these samples to circum-Antarctic detritus may suggest that a part of the detrital silicates that reaches the Bounty Trough may originate from Antarctica and has been transported in suspension in circumpolar waters and the DWBC. Where this current originates, south of the Bounty Trough, it initially decelerates because of its loss of momentum when it detaches from the ACC [Carron, 1996]. This effect could be the cause for the settling of the transported fine particles. A similar mechanism has also been invoked for sediments in the Atlantic sector of the Southern Ocean [Farrington et al., 2006].

#### 4.3.2. Open South Pacific

Figure 7 shows the Nd-Sr isotope compositions of the detrital silicate samples of this study (diamonds), excluding the samples from the New Zealand Margin (shown in Figure 6), and that of material that is likely to reach the South Pacific. These are the lithologies of the southern and austral Andes (red field), which will play an important role for the Chile Basin; dust and fine particles from Australia and New Zealand's North and South Islands (blue, yellow, and purple fields, respectively) brought by the dominant westerlies; and circum-Antarctic detritus to the south and southwest of the study area (West Antarctica, Ross Sea, and Wilkes Land; green and orange fields), from where the dominant oceanic currents may have transported this Antarctic lithogenic-derived material.

Long-distance transport from the continental sources allows only very fine-grained particles to reach these distal locations and therefore provenance rather than grain size has apparently been the most important factor controlling the Sr isotope composition of the detrital material in this area. This is also demonstrated by the significant correlation with the Nd isotope compositions of  $R^2 = 0.81$  (excluding sample 57-1, clearly affected by MORB contributions (see section 3.1)). This correlation is geographically consistent given that  $\epsilon_{Nd}$  signatures ( $^{87}Sr/^{86}Sr$  ratios) generally decrease (increase) from near South American sites toward the open ocean: Chile Basin  $>$ ( $<$ ) Chile Rise  $>$ ( $<$ ) EPR and SWP, confirming the Andes as one of the source end-members. Fine-grain dust from North Island (New Zealand) also falls in the same field as Andean rocks because of its mainly volcanic origin, but it seems less probable that its presence in the detritus increases with distance from New Zealand. Furthermore, the North Island is not under the direct influence of the westerlies as it extends into the subtropical ridge of high pressure [D , 2004] and therefore it is likely only a minor source region of detritus to the eastern South Pacific.

Besides the south and Austral Andes, a second and robust end-member cannot be clearly deduced from Figure 7 as circum-Antarctic detritus and eolian dust from Australia and South Island (NZ) display similar Sr-Nd fields. Nevertheless, almost all samples follow a trend that clearly diverges from the West Antarctica and Ross Sea detritus, except for a few samples from the Chile Basin, which may indeed have been influenced by Antarctic-derived material transported to this location by surface currents such as the Humboldt Current. Whereas, we cannot completely exclude a contribution of Sr and Nd originating from residual coatings, this is not likely in view of the efficiency of the applied leaching procedures. The apparent bowing of the mixing line is most likely simply caused by a lack of combined Sr and Nd isotope data in the Sr isotope range between 0.705 and 0.708.

Therefore, the main source candidates for the detritus arriving in the South Pacific remain Australian and South Island (NZ) dust, as suggested by other authors before [e.g., , 1994; S , 2008]. The large arid continent of Australia, the eastern part of which is affected by the westerlies that move toward the South Pacific [e.g., , 1986; H , 1994], has been even considered as the greatest contributor to atmospheric dust in the Southern Hemisphere [ C , 2006]. Central and east Australia present a huge variety of lithologies and therefore also display a large Nd-Sr field; nevertheless, the main area providing dust to the South Pacific are the Lake Eyre and Murray River Basins [ , 1989; G1 677-25

We compared authigenic and detrital core-top  $\epsilon_{\text{Nd}}$  signatures to those of bottom waters in order to identify the most reliable method to extract seawater Nd signatures from South Pacific sediments. Authigenic seawater signatures extracted from “unclean” planktonic foraminifera; fossil fish teeth and “nondecarbonated” leachates are offset to more radiogenic values from seawater  $\epsilon_{\text{Nd}}$  signatures. Independent evidence, such as REE patterns and Al/Ca measurements on “unclean” foraminifera indicate, however, that these three extraction methods effectively record bottom seawater signatures. We suggest that the observed offset between sediment and seawater Nd isotope compositions originates from the low sedimentation rates observed in this area, confirmed by  $^{14}\text{C}$  ages of up to 24 kyr. Thus, the authigenic  $\epsilon_{\text{Nd}}$  signature obtained from the core-top sediments integrates the Nd isotope signal of the Holocene and the last glacial to differing extents.

Detrital Nd and Sr isotopes indicate that the dominant sources of terrigenous material reaching the South Pacific between 35°S and 50°S are southeastern Australia and the South Island of New Zealand, the fine-grained material of which is transported by the dominant Westerlies. The influence of these two sources decreases toward the east, especially in the Chile Basin, where the detritus contains increased amounts of weathered material from the Southern and Austral Andes. Antarctica may also be a contributing source to the deposited lithogenic material of the South Pacific, especially in the domains of the Deep Western Boundary Current and the Humboldt Current.

## References

- Adams, C. J., R. J. Pankhurst, R. Maas, and I. L. Millar (2005), Nd and Sr isotopic signatures of metasedimentary rocks around the South Pacific margin and implications for provenance, *Geochimica et Cosmochimica Acta*, **69**, 2461–2476.
- Albani, S., N. Mahowald, B. Delmonte, V. Maggi, and G. Winckler (2012), Comparing modeled and observed changes in mineral dust transport and deposition to Antarctica between the last glacial maximum and current climates, *Climate Dynamics*, **38**, 1731–1755.
- Arsouze, T., J. C. Dutay, F. Lacan, and C. Jeandel (2009), Reconstructing the Nd oceanic cycle using a coupled dynamical–biogeochemical model, *Biogeochemistry*, **6**, 2829–2846.



- Elmore, A. C., A. M. Piotrowski, J. D. Wright, and A. E. Scrivner (2011), Testing the extraction of past seawater Nd isotopic composition from North Atlantic marine sediments, *Geochimica et Cosmochimica Acta*, **75**, 12, Q09008, doi:10.1016/j.gca.2011.04.011.
- Fagel, N., and N. Mattielli (2011), Holocene evolution of deep circulation in the northern North Atlantic traced by Sm, Nd and Pb isotopes and bulk sediment mineralogy, *Earth and Planetary Science Letters*, **306**, PA4220, doi:10.1016/j.epsl.2011.04.011.
- Fletcher, M.-S., and P. I. Moreno (2012), Have the Southern Westerlies changed in a zonally symmetric manner over the last 14,000 years? A hemisphere-wide take on a controversial problem, *Journal of Climate*, **25**, 253, 32–46.

- Lacan, F., and C. Jeandel (2005), Neodymium isotopes as a new tool for quantifying exchange fluxes at the continent-ocean interface, *Earth and Planetary Science Letters*, **232**, 245–257.
- Lamy, F., R. Gersonde, G. Winckler, O. Esper, A. Jaeschke, G. Kuhn, J. Ullermann, A. Martinez-Garcia, F. Lambert, and R. Kilian (2014), Increased dust deposition in the Pacific Southern Ocean during glacial periods, *Science*, **343**, 403–407, doi:10.1126/science.1245424.
- Le Fevre, B., and C. Pin (2005), A straightforward separation scheme for concomitant Lu–Hf and Sm–Nd isotope ratio and isotope dilution analysis, *Chemical Geology*, **543**, 209–221.
- Leinen, M., D. Cwienk, G. R. Heath, P. E. Biscay, V. Kolla, J. Thiede, and J. P. Dauphin (1986), Distribution of biogenic silica and quartz in recent deep-sea sediments, *Geology*, **14**, 199–203.
- Martin, E. E., and B. A. Haley (2000), Fossil fish teeth as proxies for sea water Sr and Nd isotopes, *Geochimica et Cosmochimica Acta*, **64**, 835–847, doi:10.1016/S0016-7037(99)00376-2.
- Martin, E. E., and H. D. Scher (2004), Preservation of seawater Sr and Nd isotopes in fossil fish teeth: Bad news and good news, *Earth and Planetary Science Letters*, **220**, 25–39.
- Martin, E. E., S. W. Blair, G. D. Kamenov, H. D. Scher, E. Bourbon, C. Basak, and D. N. Newkirk (2010), Extraction of Nd isotopes from bulk deep sea sediments for paleoceanographic studies on Cenozoic time scales, *Chemical Geology*, **269**.

- Roberts, N. L., A. M. Piotrowski, J. F. McManus, and L. D. Keigwin (2010), Synchronous deglacial overturning and water mass source changes, *Science*, **327**, 75–78, doi:10.1126/science.1178068.
- Roberts, N. L., A. M. Piotrowski, H. Elderfield, T. I. Eglinton, and M. W. Lomas (2012), Rare earth element association with foraminifera, *Geochimica et Cosmochimica Acta*, **94**, 57–71.
- Rosenthal, Y., M. P. Field, and R. M. Sherrell (1999), Precise determination of element/calcium ratios in calcareous samples using sector field inductively coupled plasma mass spectrometry, *Analytical Chemistry*, **71**, 3248–3253, doi:10.1021/ac981410x.
- Roy, M., T. van der Fliedt, S. R. Hemming, and S. L. Goldstein (2007),  $^{40}\text{Ar}/^{39}\text{Ar}$  ages of hornblade grains and bulk Sm/Nd isotopes of circum-Antarctic glacio-marine sediments: Implications for sediment provenance in the southern ocean, *Geochimica et Cosmochimica Acta*, **244**, 507–519.
- Rutberg, R. L., S. R. Hemming, and S. L. Goldstein (2000), Reduced North Atlantic deep water flux to the glacial Southern Ocean inferred from neodymium isotope ratios, *Earth and Planetary Science Letters*, **405**, 935–938, doi:10.1038/35016049.
- Scher, H. D., and E. E. Martin (2004), Circulation in the Southern Ocean during the Paleogene inferred from neodymium isotopes, *Earth and Planetary Science Letters*, **228**, 391–405, doi:10.1016/j.epsl.2004.10.016.